A physiologically-based framework for the simulation of skin tanning dynamics

Tenn F. Chen, Gladimir V. G. Baranoski

Tenn F. Chen, Gladimir V. G. Baranoski, "A physiologically-based framework for the simulation of skin tanning dynamics," Proc. SPIE 10877, Dynamics and Fluctuations in Biomedical Photonics XVI, 108770H (1 March 2019); doi: 10.1117/12.2504672

SPIE.

Event: SPIE BiOS, 2019, San Francisco, California, United States

A Physiologically-Based Framework for the Simulation of Skin Tanning Dynamics

Tenn F. Chen and Gladimir V. G. Baranoski

Natural Phenomena Simulation Group, School of Computer Science, University of Waterloo,
200 University Avenue West, Waterloo, Canada

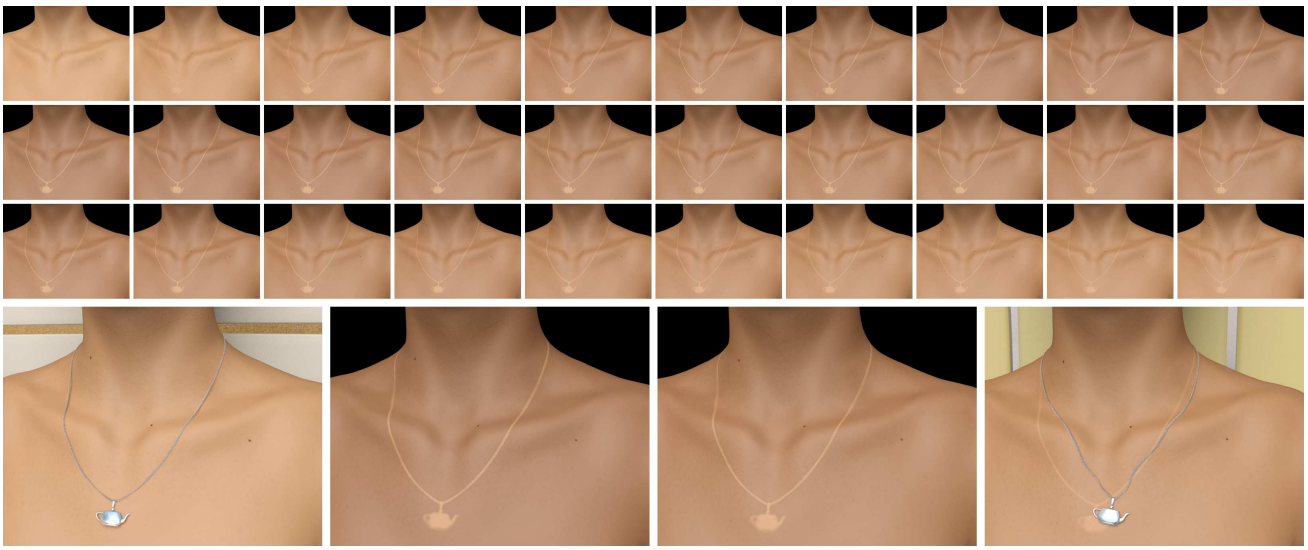

Figure 1: Frames from an animation sequence depicting simulated nonlinear appearance changes of an individual with an intermediate level of constitutive pigmentation and intermediate tanning ability (skin phototype IV as defined in Section 3). The changes, resulting from a cumulative ultraviolet radiation exposure of several hours, span a period of 30 days. The first three rows present frames (from left to right, top to bottom) depicting the sequence of daily changes. The bottom row presents selected frames (from left to right) showing the initial pigmentation level, the peak pigmentation level at day 10 and faded pigmentation levels at days 20 and 30. These frames were generated using the data provided in Tables 1 (dataset $\mathcal{I}$), 2 and 3.

ABSTRACT

A comprehensive understanding about the dynamics of time-dependent, photoinduced physiological processes affecting the spectral attributes and, consequently, the appearance of human tissues is essential for new advances in biology, medicine, biomedical photonics and computer graphics, just to name a few fields that can benefit from it. Skin is arguably the most investigated of these complex biological systems. Its interactions with light have been the object of extensive studies aimed at a wide range of applications, from the detection and treatment of diseases to the synthesis of realistic images for educational and entertainment purposes. However, the dynamics of photoinduced physiological processes leading to skin appearance changes over time remains an open research topic. In this paper, we address the effects of tanning, one of the most prominent and persistent photobiological phenomena leading to such appearance changes. More specifically, we present a novel physiologically-based framework for the simulation of skin tanning dynamics, and describe how it can be employed in the visualization of the tanning-induced variations on skin's spectral attributes. Its first-principles algorithms explicitly account for the connections between spectrally-dependent light stimuli and time-dependent physiological reactions occurring within the cutaneous tissues. This enables the effective simulation of these tissues' main mechanisms of adaptation to ultraviolet radiation. As a result, nonlinear skin appearance changes elicited by distinct light exposure regimes

Further author information: send correspondence to Gladimir V. G. Baranoski (E-mail: gvgbaran@cs.uwaterloo.ca).

Dynamics and Fluctuations in Biomedical Photonics XVI, edited by Valery V. Tuchin, Martin J. Leahy, Ruikang K. Wang
Proc. of SPIE Vol. 10877, 108770H · © 2019 SPIE · CCC code: 1605-7422/19/$18 · doi: 10.1117/12.2504672

can be correctly reproduced. We demonstrate the predictive capabilities of the proposed framework through quantitative and qualitative comparisons of its outcomes with measurements and experimental observations reported in the literature. We believe that it provides a high-fidelity testbed for interdisciplinary research involving time-dependent skin responses to light exposure.

Keywords: photobiological phenomena, skin appearance changes, ultraviolet radiation, spectrally-dependent light stimuli, time-dependent physiological processes.

1. INTRODUCTION

Tanning is responsible for some of the most common and visually striking appearance changes observed in human skin. It is a complex time-dependent phenomenon characterized by a nonlinear relationship between the triggering external stimuli and the resulting effects on skin appearance.[1,2] This aspect is accentuated by the fact that additional external stimuli can still be applied while the underlying physiological mechanisms are already in progress.[3]

Clearly, one can resort to standard techniques, such as interpolations guided by *ad hoc* control curves, to mimic temporal variations on the biophysical parameters (*e.g.*, epidermal melanin content and tissue thickness) associated with skin appearance changes. We note, however, that situations directly connected to the time-dependent and nonlinear characteristics of tanning cannot be predictively addressed using such techniques. For example, when does the darkening appearance of skin reach a steady state plateau in response to ultraviolet radiation (UVR) exposure? For how long does the plateau last? How does the exposure dose affect the timing and duration of a tan already in progress? How does it affect a tan that is already fading?

Motivated by these aspects, we present a novel comprehensive framework for the physiologically-based simulation and visualization of time-dependent skin appearance changes resulting from tanning elicited by UVR exposure. It is important to note that we are not proposing yet another model of light and skin interactions. Although we employ available models, notably in the visualization of simulation results, our research described here focuses on skin appearance dynamics. Accordingly, its main purpose is the predictive computation of temporal variations in skin biophysical parameters. To achieve this capability, it involved primarily the development of simulation algorithms whose central formulations, albeit built on the current physiological understanding about skin tanning, were originally devised during this work.[6]

Tanning encapsulates the two main adaptive mechanisms developed by human skin to guard against the harmful effects of UVR, namely stimulation of melanin synthesis[1] and tissue thickening (hyperplasia).[5] Within the proposed framework, these mechanisms are simulated using a first principles approach that accounts for the distinct degrees of UVR sensitivity of different individuals and the effectiveness of distinct UVR wavelengths at eliciting tanning responses. We demonstrate the predictive capabilities of the proposed framework by quantitatively and qualitatively comparing its outcomes with measurements and observations reported in the scientific literature. In these comparisons, we include image sequences depicting nonlinear and time-dependent appearance changes resulting from tanning processes guided by different levels of adaptation to UVR exposure.

To the best of our knowledge, the comprehensive physiologically-based simulation and visualization of skin tanning dynamics has not been addressed in the scientific literature prior to this work.[6] Although mathematical descriptions of skin pigmentation mechanisms have been proposed in the biomedical field,[7,8] they neither consider the different responses triggered by distinct UVR exposure regimes,[3,9] nor directly address the broad range of UVR sensitivity observed in the human population.[10–12] Moreover, although these works acknowledge the influence of skin thickness on tanning responses, they do not account for the hyperplasia mechanism.[5,13,14]

It is worth noting, however, that one can find a relative large number of publications on the simulation and visualization of short and long term skin appearance changes.[15] Publications in the former group tend to focus on changes elicited by variations in dermal blood parameters,[16] which may be associated with medical conditions such as anemia,[17] cyanosis[18–20] and jaundice.[21] Publications in the latter group, on the other hand, tend to focus on changes resulting from aging related phenomena, such as the formation of folds and wrinkles,[22] or pathological process such as the development of skin pigmentation disorders.[23] These works, however, do not directly incorporate the connections between the external stimuli and the corresponding time-dependent physiological mechanisms. When the effects of external factors (*e.g.*, light exposure) over time are simulated,[24]

this is usually done in a passive manner, *i.e.*, simply using a time variable to perform an *ad hoc* modulation of skin biophysical parameters.

In the case of tanning, these stimulus-response connections can be illustrated, for example, by the mechanisms involving melanin's redistribution and degradation.[25] These physiological reactions, which vary according to the duration, intensity and spectral distribution of the light stimuli,[26,27] lead to skin appearance changes (Figure 2) that are proportional to the individual's native level of adaptation to UVR exposure.[10] The proposed framework takes these factors as explicit input data to the dynamics simulations.

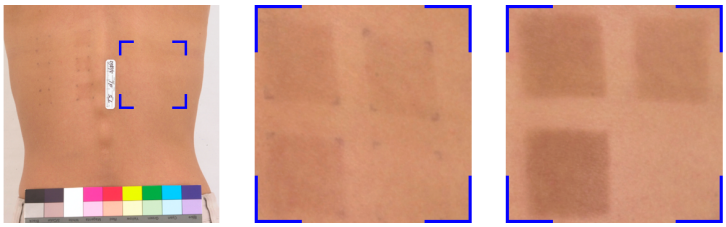

Figure 2: Photograph series showing changes in pigmentation over time as a result of a controlled tanning experiment using distinct UVR exposure doses.[9] Left: initial state. Center: emerging responses. Right: peak responses. The three patches of darkened skin correspond to different exposure doses, and the fourth patch (on the lower right of center and right images) represents the unexposed control area. Note that areas on the left side of the back (leftmost photo) show results from previous experiments on skin sensitivity to UVR exposure. Courtesy of S. Miller. Original image copyright by John Wiley & Sons, Inc.

From a broader scientific perspective, the proposed framework can serve as a platform for the *in silico* investigation of spectrally-dependent photobiological phenomena affecting skin appearance over time. For example, using the proposed framework, one can perform controlled simulations (*e.g.*, considering specific light exposure conditions and individuals with distinct biophysical characteristics) involving these phenomena. The results of these simulations can be used in the production of computer animations, which, in turn, can be employed as a means to gain further insights into these phenomena through the visualization of their effects under different experimental conditions.

It is also worth noting that the realistic and automatic (without careful manual tweaks by artists and experts) rendering of biological materials remains a challenging topic in computer graphics. This is particularly the case of virtual human characters employed in a wide range of educational and entertainment applications, from movies and games to virtual reality productions. Since the human visual system is finely tuned to detect subtle variations in their appearance, the proposed framework can contribute to enhance their perceived level of realism by providing important cues associated with ubiquitous tanning effects. The use of these visual cues, obtained through predictive simulations guided by physiologically meaningful parameters, would represent another step toward a more automatic rendering of virtual human characters.

The remainder of this paper is organized as follows. We provide a concise review of relevant photobiological background in Section 2. In Section 3, we describe the proposed algorithms for the simulation of skin tanning dynamics. We then present the results of this research and discuss relevant practical issues in Section 4. Finally, we conclude the paper and outline directions for future work in Section 5.

2. PHOTOBIOLOGICAL BACKGROUND

The intrinsic optical properties of human skin and their connection with its appearance have been extensively examined in previous works in this area.[4,15] For this reason, in this section, we primarily review photobiological concepts and terminology relevant for this research on skin tanning dynamics.

The two most visible skin responses to excessive UVR exposure are *erythema* (commonly known as "sunburn") and *tanning*.[28] The former results from a vasodilation of the dermal blood vessels,[29] which leads to skin reddening at the stimulus site. It is worth mentioning that this chromatic variation can also be triggered by mechanical, chemical, electrical and thermal stimuli.[30,31] Compared to tanning, however, erythema can be considered a fleeting phenomenon.[28] Furthermore, the occurrence of erythema, notably in individuals with low

tanning ability,[32] is often associated with blistering and peeling. The correct reproduction of such extreme morphological changes would require alterations in the skin structure that are beyond the scope of this research. For these reasons, erythema is further addressed in this work only when referring to specific physical quantities employed in the simulation of tanning dynamics.

During UVR exposure, a reduction in the skin tissues' water content may take place. It has been demonstrated,[33] however, that water losses predominantly affect skin spectral responses in the infrared domain. In the ultraviolet and visible domains, the attenuation of light is largely dominated by melanin, more specifically the two main types of this pigment found in the cutaneous tissues, namely the more abundant brown-black eumelanin and the yellow-red pheomelanin.[28,34] Hence, the impact of water losses on the visible reflectance of tanned skin is negligible.[35] For this reason, it is not further addressed in this research.

The melanin pigmentary system's photobiology involves several phenomena.[1,27] The most relevant, known as delayed tanning, is responsible for the familiar long-lasting tan induced by UVR exposure,[28] the focal point of this research. The effects of this phenomenon, henceforth referred to as the tanning process, are usually visible about 24 hours after sufficient UVR exposure, and they can last anywhere from days to more than a year.[28,36,37]

The tanning process is mainly characterized by an increase in the skin pigmentation level, which is directly associated with an increased presence of melanin. This pigment is typically found within the epidermal layers in colloidal and aggregated forms. In the latter case, it is encapsulated within organelles called melanosomes.[28] It is important to note that the perceived level of cutaneous pigmentation of an individual and the amount of UVR absorbed by his/her skin depend not only on the quantitative presence of melanin in his/her epidermis, but also on its distribution patterns within this tissue.[1,26–28,38,39]

Melanin is synthesized, through a phenomenon termed melanogenesis, by cells known as melanocytes, which are mostly concentrated in the innermost epidermal layers. Melanin, notably in aggregated form, is spread throughout the full thickness of the epidermis as the skin cells migrate upwards towards the surface (Figure 3).[40] During tanning, there is an increase in the number and activity of melanocytes.[1] Besides shifting the distribution of melanin within the epidermis,[25] these processes lead to an increase in the amount of this pigment found in this tissue. This increase in melanin content is known as facultative pigmentation, while the original baseline pigmentation level (induced by genetic factors) is known as constitutive pigmentation.[28] Additionally, the thickness of both epidermis and dermis is subjected to change during tanning through the hyperplasia mechanism.[5,28,41]

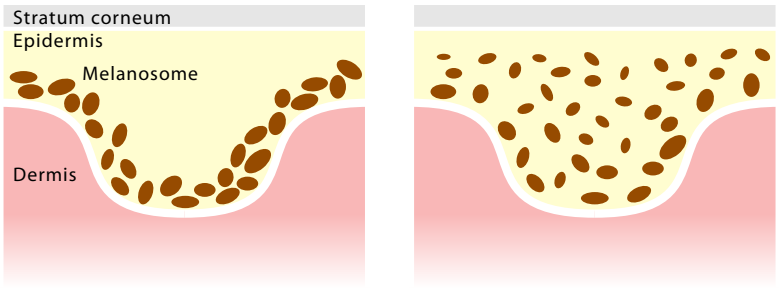

Figure 3: Sketches illustrating the distribution of melanin within the epidermis. Left: initially the melanin encapsulated within the melanosomes is predominantly located within the innermost epidermal layers. Right: as the epidermal cells migrate upwards, melanin is distributed throughout the epidermis.

The level of adaptation to UVR exposure varies among distinct skin specimens (skin samples belonging to different individuals), and it has been used to establish the Fitzpatrick skin phototype (SPT) classification.[32] According to this classification, among specimens with a low constitutive pigmentation level, there are those that cannot tan (SPT I), and those that have this ability in different degrees (SPT II, III and IV). In addition, specimens characterized by an intermediate or high constitutive pigmentation level (SPT V and VI, respectively) are capable of tanning profusely and rarely show signs of erythema.[32] Although this classification can be used to qualitatively describe the typical tanning responses of different skin specimens, it has been pointed out that there is no clear quantitative relationship between skin phototype and ultraviolet sensitivity.[10,42]

Alternatively, Ravnbak *et al.*[10] quantitatively related skin pigmentation to the minimum erythema dose (MED) and minimum melanogenesis dose (MMD). Both quantities are measured in terms of J/m^2, and they are defined as the minimum amount of radiant energy per unit area necessary to produce visually perceptible erythema and tanning responses, respectively.[2] These quantities have been associated with analogous expressions, namely optical energy density,[43] radiant exposure[44] or exposure dose.[11,45] We employ the latter in this document for consistency with seminal supporting references. Both quantities are often provided in terms of the standard erythema dose (SED),[46] and they are denoted as MMD_{SED} and MED_{SED} in this work. According to CIE (Commission Internationale de l'Eclairage),[47] a unit of SED (employed as a reference in tanning experiments[10]) is defined as 100 J/m^2 at 298 nm. This wavelength was selected by CIE for being the most effective wavelength at eliciting photobiological responses (*e.g.*, erythema and melanogensis) to UVR exposure.[46,47]

The study and analysis of a given photobiological phenomenon often requires the knowledge about the action spectrum of the physiological mechanisms associated with this phenomenon. This property is defined as the relative effectiveness of different wavelengths of light in triggering a specific phenomenon[11] and it is expressed in terms of arbitrary units (a.u.). In this research, we take into account the action spectra of melanogenesis and erythema (Figure 4), denoted by α_m and α_e, respectively. While the former is employed in computations involving melanin production, the latter is used in computations associated with the regulation of skin thickness. These computations are described in Section 3.1. We note that action spectra depicted in Figure 4 are normalized at 298 nm. This wavelength is used by CIE as the normalization reference for action spectra also on the account of its effectiveness to elicit photobiological responses.[46,47]

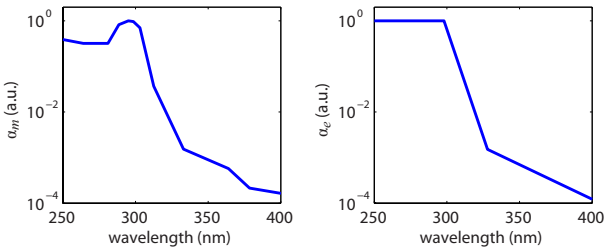

Figure 4: Action spectra of melanogenesis[11] (left) and erythema[48] (right) expressed in arbitrary units (a.u.).

3. FRAMEWORK DESCRIPTION

The proposed framework takes as input the UVR exposure doses and the initial values for the biophysical parameters that characterize a given skin specimen. It employs an algorithmic formulation organized into modules (Figure 5). Accordingly, the simulations of the main tanning mechanisms, namely melanogenesis and hyperplasia, are carried out in the melanin dynamics and thickness dynamics modules, respectively. Within these modules, the UVR exposure doses are initially evaluated (Section 3.1) to determine whether they are sufficient to elicit time-dependent variations in melanin pigmentation and skin thickness. These variations can then be simulated (Sections 3.2 and 3.3) to yield the corresponding changes in the specimen's characterization parameters.

A discrete time-stepping method is used in the implementation of the simulations outlined above. It can account for single or multiple exposure doses of distinct intensities as well as arbitrary illumination geometries. Different time-steps (*e.g.*, Δt equal to 1 hour or 1 day) can be selected according to the application at hand. We remark that the formulations presented in this section were originally developed for this research, albeit being grounded on the current knowledge about the underlying physiological mechanisms of skin tanning. Moreover, unless otherwise stated, the variables employed in these formulations refer to relative values (expressed in a.u.).

3.1 UVR Dose Evaluation

For both the melanin dynamics and thickness dynamics modules, we start by calculating the UVR threshold at which the corresponding physiological mechanism is activated for a skin specimen. These quantities, referred to as the melanogenesis threshold and hyperplasia threshold, are denoted by $\Psi_\circ$ and $\Psi'_\circ$, respectively. They are

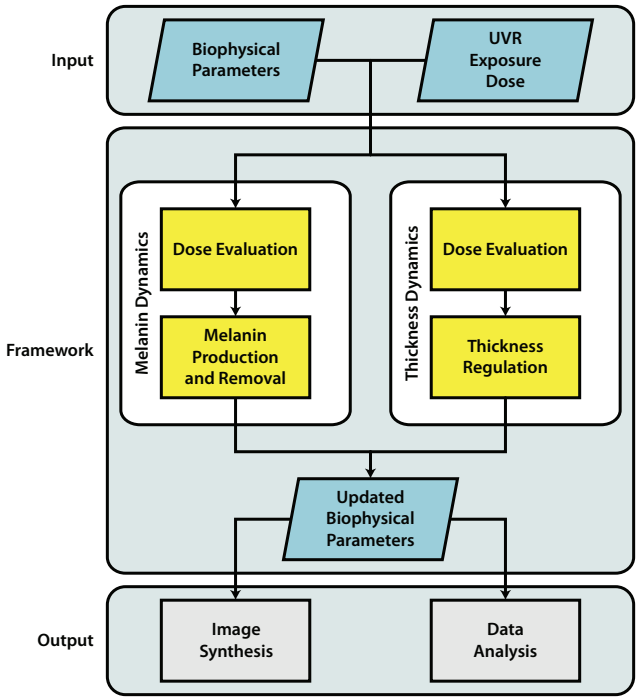

Figure 5: Diagram depicting the modular structure of the proposed framework for the physiologically-based simulation of skin tanning dynamics. The detailed description of the tasks associated with each module is provided in Sections 3.1 to 3.4.

calculated using the following expressions:

$$\Psi_\circ = \int_\lambda \alpha_m(\lambda)\, \psi_\circ(\lambda)\, A(\lambda)\, \mathrm{d}\lambda \tag{1}$$

and

$$\Psi'_\circ = \int_\lambda \alpha_e(\lambda)\, \psi'_\circ(\lambda)\, A(\lambda)\, \mathrm{d}\lambda, \tag{2}$$

where $\psi_\circ$ and $\psi'_\circ$ correspond to the spectral MMD and the spectral MED, respectively, and $A(\lambda)$ represents the specimen's spectral absorptance (absorbed fraction of the impinging light[15]). Note that the α_m and α_e are plotted in Figure 4. In addition, we employ the latter in the evaluation of $\Psi'_\circ$ since it has been indicated that changes in skin thickness are related to erythema responses.[5]

As outlined in Section 2, the amount of absorbed UVR is markedly affected by the quantitative presence and distribution patterns of melanin (in its distinct forms) found within the epidermal layers.[1,26–28,38,39] Accordingly, the spectral absorptance is computed using a model of light and skin interactions that can provide predictive results in the ultraviolet domain by carefully accounting for these aspects. Due to its modular structure (Figure 5), the proposed framework can be effectively implemented using any model that satisfies this requirement. We elected to use the HyLIoS (*Hy*perspectral *L*ight *I*mpingement *o*n *S*kin) model[4] not only because it satisfies this requirement, but also because it provides outputs (which can be obtained using its online version[49]) that exhibit a high degree of fidelity. In fact, HyLIoS has been successfully employed in a number of biomedical investigations.[17–20,50]

Recall that to elicit a physiological response, a minimum dose is required, and this dose may be administered at a single or multiple wavelengths.[2] Thus, the MMD_{SED} can elicit the same tanning response that would be triggered by a spectral MMD.[51] Also recall that the erythema and melanogenesis action spectra (Figure 4) are normalized at 298 nm (Section 2). Hence, we can simplify the calculation of the melanogenesis threshold to yield:

$$\Psi_\circ = \alpha_m(298)\, MMD_{SED}\, A(298). \tag{3}$$

Note that α_m and A are evaluated at 298 nm for consistency with MMD_{SED}. A similar procedure using α_e and MED_{SED} can be performed for the calculation of $\Psi'_\circ$.

It is important to consider that a specimen may be subjected to multiple UVR exposure doses. Hence, in order for melanogenesis and hyperplasia to be triggered, the total UVR intake accumulated for these mechanisms must be equal to or larger than their corresponding thresholds. This triggering procedure, which is associated with the production of a signal substance for the respective mechanism,[26, 52] is implemented as follows.

For each received UVR exposure dose, we calculate the corresponding UVR intake for the melanogenesis and hyperplasia mechanisms. These two quantities, denoted by $\Psi(t)$ and $\Psi'(t)$, respectively, are obtained using the following expressions:

$$\Psi(t) = \int_\lambda \alpha_m(\lambda)\, \psi(\lambda, t)\, A(\lambda)\ \mathrm{d}\lambda \tag{4}$$

and

$$\Psi'(t) = \int_\lambda \alpha_e(\lambda)\, \psi(\lambda, t)\, A(\lambda)\ \mathrm{d}\lambda, \tag{5}$$

where $\psi(\lambda, t)$ represents the spectral (radiant) exposure dose received by the skin specimen at time t.

Note that the dose received at time t needs to be associated with the specimen's MMD (for the melanin dynamics simulation) or MED (for the thickness dynamics simulation). Accordingly, the corresponding normalized UVR intakes, denoted by $d(t)$ and $d'(t)$, respectively, are expressed as:

$$d(t) = \frac{\Psi(t)}{\Psi_\circ} \tag{6}$$

and

$$d'(t) = \frac{\Psi'(t)}{\Psi'_\circ}. \tag{7}$$

The normalized UVR intakes retained within the skin, which can lead to melanogenesis and hyperplasia, are denoted by $e_\circ(t)$ and $e'_\circ(t)$, respectively. They are expressed as:

$$e_\circ(t) = d(t) + e_\circ(t - \Delta t)\delta_{e_\circ}, \tag{8}$$

and

$$e'_\circ(t) = d'(t) + e'_\circ(t - \Delta t)\delta_{e'_\circ}, \tag{9}$$

where $\delta_{e_\circ} \in [0, 1]$ and $\delta_{e'_\circ} \in [0, 1]$ represent the decays of $e_\circ(t)$ and $e'_\circ(t)$, respectively.

Signal substances[26, 52] may then be produced, prompting the melanogenesis and hyperplasia mechanisms. The rate of production of these signal substances, denoted by $s_\circ(t)$ and $s'_\circ(t)$, respectively, can be related to the retained normalized UVR intake as:

$$s_\circ(t) = e(t) + s_\circ(t - \Delta t)\delta_{s_\circ}, \quad \text{with} \tag{10}$$

$$e(t) = \begin{cases} 0 & \text{when } e_\circ(t) < 1 \\ e_\circ(t) & \text{otherwise,} \end{cases} \tag{11}$$

and

$$s'_\circ(t) = e'(t) + s'_\circ(t - \Delta t)\delta_{s'_\circ}, \quad \text{with} \tag{12}$$

$$e'(t) = \begin{cases} 0 & \text{when } e'_\circ(t) < 1 \\ e'_\circ(t) & \text{otherwise,} \end{cases} \tag{13}$$

where $\delta_{s_\circ} \in [0,1]$ and $\delta_{s'_\circ} \in [0,1]$ correspond to the decays of $s_\circ(t)$ and $s'_\circ(t)$, respectively. Recall that melanogenesis and hyperplasia responses occur only when the relevant accumulated UVR intakes are equal to or larger than the corresponding thresholds. The definitions of $e(t)$ and $e'(t)$ provided above incorporate these triggering conditions.

The actual amounts of the signal substances for melanogenesis and hyperplasia produced at a time t, denoted by $s(t)$ and $s'(t)$, respectively, can then be expressed as:

$$s(t) = s_\circ(t) + s(t - \Delta t)\delta_s \tag{14}$$

and

$$s'(t) = s'_\circ(t) + s'(t - \Delta t)\delta_{s'}, \tag{15}$$

where $\delta_s \in [0,1]$ and $\delta_{s'} \in [0,1]$ are the decays of the signal substances for melanogenesis and hyperplasia, respectively.

3.2 Melanin Dynamics Simulation

In this section, we describe how we simulate the changes in melanin content and distribution. The corresponding formulation used to simulate these changes was developed considering experimental observations and theoretical insights provided by studies on the skin facultative pigmentation mechanism.[1,8,25,51]

The two forms of melanin found in the human skin, namely eumelanin and pheomelanin, are treated in the same way during the melanin dynamics simulations since their proportions are known to remain relatively constant following UVR exposure.[27,53] However, their proportions within the epidermal layers are accounted for in the computation of the resulting skin appearance attributes (Section 3.4). In addition, for consistency with the related literature, the volume fraction, or percentage, of a given layer occupied by melanin is expressed in terms of melanin content, and denoted by m. Similarly, the relative amount of melanin found in a given epidermal layer with respect to the total amount of melanin found in all epidermal layers is expressed in terms of relative melanin content, and denoted by $\hat{m}$.

Melanin can be introduced into the three main epidermal layers, namely stratum basale (layer 1), stratum spinosum (layer 2) and stratum granulosum (layer 3), in two ways: produced directly within each layer by melanocytes through melanogenesis or transferred upwards from the layer below through epidermal cell migration.[40] Furthermore, melanin can be removed from each layer in two ways: degraded naturally or transferred upwards to the layer above.[8] A diagram illustrating these processes is presented in Figure 6.

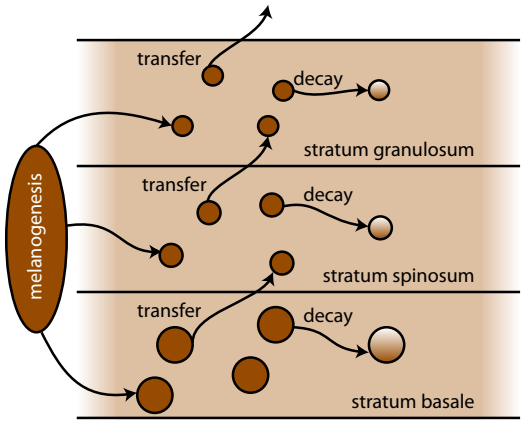

Figure 6: Two-dimensional diagram illustrating the melanin production and removal processes considered in our melanin dynamics simulations. The dark brown circles represent melanosomes (three-dimensional organelles containing melanin). The smaller dark brown circles in the upper layers represent smaller melanosomes found in the upper layers of skin. The lighter brown circles represent melanosomes encapsulating degraded melanin.

We express the melanin production rate in a given layer i (with $i = 1, 2, 3$) as:

$$m_{p,i}(t) = M(t)\, m_{p,i,f} + m_{p,i,c}, \tag{16}$$

and the fraction of melanin transferred from layer i to the layer above as:

$$m_{t,i}(t) = M(t)\, m_{t,i,f} + m_{t,i,c}, \tag{17}$$

where $m_{p,i,c}$ and $m_{t,i,c}$ represent the constitutive melanin production and transfer rates for layer i, respectively, $m_{p,i,f}$ and $m_{t,i,f}$ correspond to the increase in facultative melanin production and transfer rates, respectively, and $M(t)$ is a factor used to modulate the facultative melanin production and transfer rates. This factor is a function of the amount of signal substance (Equation 14), with a larger amount increasing the physiological responses up to an equilibrium level. It is expressed in terms of the Hill function for physicochemical equilibrium[54] as:

$$M(t) = \frac{s^{\kappa}(t)}{s^{\kappa}(t) + \omega^{\kappa}}, \tag{18}$$

where κ and ω correspond to the Hill coefficients associated with the effectiveness of the signal substance regulating the melanogenesis mechanism. The relative melanin content in layer i is given by:

$$\begin{aligned} \hat{m}_i(t) = {} & m_{p,i}(t) + \\ & \delta_m(1 - m_{t,i}(t - \Delta t))\, \hat{m}_i(t - \Delta t) + \\ & m_{t,i}(t - \Delta t)\, \hat{m}_{i-1}(t - \Delta t), \end{aligned} \tag{19}$$

where δ_m is the fraction of melanin that remains after its degradation. Since there is no layer below the stratum basale capable of transferring melanin upwards, the third term of Equation 19 can be omitted when applied to the stratum basale.

At time $t = 0$, $\hat{m}_i(t)$ corresponds to the steady state. Thus, if there is no tanning, then $\hat{m}_i(0) = \hat{m}_i(t)$ for any t. Similarly, $m_{p,i}(t) = m_{p,i,c}$ and $m_{t,i}(t) = m_{t,i,c}$. Hence, the steady state value for layer i can be written as:

$$\hat{m}_i(0) = \begin{cases} \dfrac{m_{p,i,c}}{1 - \delta_m(1 - m_{t,i,c})} & \text{when } i = 1 \\ \dfrac{m_{p,i,c} + m_{t,i-1,c} m_{i-1}}{1 - \delta_m(1 - m_{t,i,c})} & \text{otherwise.} \end{cases} \tag{20}$$

We remark that Equation 19 is used to describe the relative melanin content between the different layers in relation to the initial content. That is, the sum of melanin contents assigned to the three layers at time $t = 0$ is equal to 1, and the total normalized change in melanin pigmentation at time t can be calculated as:

$$\Delta\hat{m}(t) = \sum_{i=1}^{3} \hat{m}_i(t). \tag{21}$$

Accordingly, the fraction of total melanin located in layer i at time t is given by $\hat{m}_i(t)/\Delta\hat{m}(t)$. Thus, for each layer i at time t, the updated melanin content can be evaluated as:

$$\begin{aligned} m_i(t) = {} & \text{epidermal melanin pigmentation increase at time } t \times \\ & \text{proportion of total melanin in layer } i \text{ at time } t \times \\ & \text{original epidermal melanin pigmentation content} \div \\ & \text{proportion of epidermis occupied by layer } i \\ = {} & \Delta\hat{m}(t) \frac{\hat{m}_i(t)}{\Delta\hat{m}(t)} \left[\sum_{\iota=1}^{3} \left(\frac{\bar{m}_\iota \tau_\iota}{\tau_e} \right) \right] \left[\frac{\tau_i}{\tau_e} \right]^{-1} \qquad (22) \\ = {} & \frac{\hat{m}_i(t)}{\tau_i} \sum_{\iota=1}^{3} \left(\bar{m}_\iota \tau_\iota \right), \qquad (23) \end{aligned}$$

where $\bar{m}_i$ is the original melanin content for layer i, τ_i corresponds to the original thickness of layer i, and τ_e represents the original thickness of the epidermis, *i.e.*, the sum of τ_1, τ_2 and τ_3.

3.3 Thickness Dynamics Simulation

In this section, we describe how we simulate the changes in skin thickness. The formulation employed to simulate these changes was developed considering primarily experimental observations reported in studies about hyperplasia.[5,13] According to these studies, in contrast to melanogenesis, hyperplasia is not limited to the epidermis.[5,13] We remark, however, that both adaptive mechanisms are dependent on UVR exposure.[1] Hence, we employ a similar algorithmic approach in their simulations.

The regulation of skin thickness is assumed to be the result of two competing processes: the generation and loss of skin cells. The generation of skin cells, denoted as τ_p, can be formulated as:

$$\tau_p(t) = M'(t)\,\tau_{p,tan} + \tau_{p,base}, \tag{24}$$

where $\tau_{p,base}$ represents the baseline skin cell production rate, $\tau_{p,tan}$ corresponds to the increase in this production rate, and $M'(t)$ is a factor that modulates the effect of this increase. Analogous to the melanogenesis mechanism, this factor is a function of the amount of the corresponding signal substance (Equation 15), and it is expressed as:

$$M'(t) = \frac{s'^{\kappa'}(t)}{s'^{\kappa'}(t) + \omega'^{\kappa'}}, \tag{25}$$

with κ' and ω' representing the Hill coefficients[54] employed for the hyperplasia mechanism. The actual skin thickness is then given by:

$$\tau(t) = \tau_p(t) + \tau(t - \Delta t)\delta_\tau, \tag{26}$$

where $\delta_\tau \in [0, 1]$ accounts for the loss in skin cells. At time $t = 0$, $\tau(t)$ corresponds to the steady state:

$$\tau(0) = \frac{\tau_{p,base}}{1 - \delta_\tau}. \tag{27}$$

Finally, the normalized thickness change at time t is given by:

$$\Delta\tau(t) = \frac{\tau(t)}{\tau(0)}. \tag{28}$$

As mentioned earlier, the thickness regulation algorithm computes the change in thickness for the entire skin. Hence, at time t, one needs to scale the original values assigned to each skin layer by $\Delta\tau(t)$. In addition, recall that melanin content is expressed in terms of volume fraction. Accordingly, to avoid inadvertently altering the amount of melanin present in the epidermis when scaling the thickness, one needs to divide the melanin content of each of its layers by $\Delta\tau(t)$.

3.4 Framework Output

Once the dynamics simulations are completed, the values for the updated biophysical parameters (*e.g.*, epidermal melanin content and tissue thickness) can be employed in data-driven investigations of photobiological phenomena affecting human skin (Figure 5). Alternatively, they can be used as input to a model of light and skin interactions in order to enable the computation of skin appearance attributes (*e.g.*, spectral reflectance and bidirectional scattering-surface reflectance distribution function (BSSRDF)[15]). These attributes can then be employed in the synthesis of images portraying the resulting skin appearance changes (Figure 5). These images, in turn, can be used in the production of animation sequences depicting tanning variations on virtual human characters over time.

For consistency, one can employ the same model used in the evaluation of UVR exposure doses (Section 3.1). In the case of HyLIoS,[4] we note that it takes into account the distribution of melanin in colloidal and aggregated forms in the different epidermal layers. Accordingly, if this model is employed, then the changes in melanin content resulting from the dynamics simulations are applied to the contents of both forms of melanin found in

each of these layers. In addition, their original proportions (used in the characterization of the specimen at hand) are maintained during this operation.

It is worth stressing that the translation of simulation results to skin appearance attributes is not tied to a specific model. For example, if one wants to employ a model in which the epidermis is represented by a single layer (*e.g.*, the BioSpec (*Bio*physically-based *Spec*tral) model[16]), the epidermal melanin content can be scaled by $\Delta\hat{m}$ (Equation 21). As for the eumelanin to pheomelanin ratio, we remark that it remains mostly constant during tanning.[9,53]

As mentioned above, animations showing skin appearance changes over time can be produced by employing the updated parameter values provided by the framework at every time step. These are then translated to skin appearance attributes by the selected model of light and skin interactions and incorporated to the rendering algorithm of choice. For example, all synthetic images presented in this paper, with the exception of the skin swatches depicted in Figure 15, were rendered using a ray tracing algorithm and three-dimensional geometrical models of human characters. In the case of features like tan lines, their rendering can be performed by taking advantage of the contrast provided by the original and modified appearance attributes. For the skin swatches presented in Section 4.2, the skin appearance attributes were converted to skin tone values using a standard XYZ to sRGB conversion procedure[55] and considering the white point coordinates associated with a standard CIE D65 illuminant.[56] After this conversion, we applied a greyscale skin texture to the swatches.

4. RESULTS AND DISCUSSION

In this section, we evaluate the predictive capabilities of the proposed framework and demonstrate its applicability to the reproduction of skin appearance changes resulting from tanning processes triggered by different UVR exposure conditions. We also address practical issues related to its evaluation and use.

4.1 Tanning Dynamics Specification Data

We considered time-steps of 1 hour in the simulations reported in Section 4.2. Unless otherwise indicated, their results were translated to skin appearance attributes (Figure 5) using the HyLIoS model, whose algorithms and default (baseline) parameter values are provided in the original publication describing this model.[4] These simulations were controlled by biophysical parameters listed in Tables 1 to 3. Their values were obtained from experimental measurements[5,25] using standard estimation procedures also employed in related works.[7,8] A detailed description of these procedures is provided elsewhere[6] for conciseness.

For some parameters depicted in Table 1, one can observe that, in certain instances, their values with respect to a high level of constitutive pigmentation were lower than those assigned for a low level of constitutive pigmentation. We remark that some of these parameters are associated with melanin transfer rates. In other words, their lower values correspond to a higher retention of melanin, which, in turn, can lead to a higher overall content of this pigment in the respective epidermal layer. We also note that for specimen-dependent parameters, such as those listed in Table 1, these figures may be adjusted to describe individuals with lower or higher tanning ability.

Since morphological changes observed in an individual's skin tissues over the years can be translated to different values for specific biophysical parameters (*e.g.*, thickness), we used these parameters to guide the simulations instead of an individual's age. We note that in controlled tanning experiments involving subjects belonging to different age groups,[3] no significant tanning trend specifically associated with age was noticed.

4.2 Quantitative and Qualitative Comparisons

Initially, we assessed the capability of the proposed framework to account for a phenomenon directly connected to tanning responses. More specifically, we tested its predictions with respect to photoaddition and arbitrary UVR exposure dose schedules. Photoaddition is the phenomenon where multiple smaller exposure doses yield a physiological response similar to one from a larger single dose.[57] As it can be observed in Figure 7, while each of the small doses independently produces a smaller pigmentation response (a smaller percentage increase in melanin content), in combination, they produce a response similar to that of the single large dose.

epidermal layer	parameter	constitutive pigmentation level $\mathcal{L}$	$\mathcal{I}$	$\mathcal{H}$
stratum granulosum	$m_{p,i,c}$	0.0000	0.0000	0.0000
	$m_{t,i,c}$	0.0004	0.0064	0.0003
	$m_{p,i,f}$	0.0000	0.0000	0.0000
	$m_{t,i,f}$	0.0000	0.0900	0.0700
stratum spinosum	$m_{p,i,c}$	0.0000	0.0030	0.0020
	$m_{t,i,c}$	0.0051	0.0090	0.0029
	$m_{p,i,f}$	0.0000	0.0150	0.0065
	$m_{t,i,f}$	0.0200	0.0010	0.0010
stratum basale	$m_{p,i,c}$	0.0100	0.0080	0.0080
	$m_{t,i,c}$	0.0081	0.0051	0.0018
	$m_{p,i,f}$	0.0110	0.0075	0.0085
	$m_{t,i,f}$	0.0450	0.0250	0.0300

Table 1: Values for constitutive pigmentation dependent parameters employed in the melanin dynamics simulations (Section 3.2). The three parameter datasets associated with distinct constitutive pigmentation levels, namely $\mathcal{L}$ (Low), $\mathcal{I}$ (Intermediate) and $\mathcal{H}$ (High), are based on experimental measurements performed by Tadokoro *et al.*[25]

parameter	$\delta_{e_\circ}$	$\delta_{s_\circ}$	δ_s	δ_m	κ	ω
value	0.98	0.99	0.985	0.99	0.7	500

Table 2: Values for constitutive pigmentation independent parameters employed in the melanin dynamics simulations (Section 3.2). The estimation of these values was based on data from actual tanning experiments performed by Tadokoro *et al.*[25]

parameter	$\delta_{e'_\circ}$	$\delta_{s'_\circ}$	$\delta_{s'}$	δ_τ	κ'	ω'	$\tau_{p,base}$	$\tau_{p,tan}$
value	0.985	0.2	0.98	0.9	1	20	0.1	0.025

Table 3: Values for constitutive pigmentation independent parameters employed in the thickness dynamics simulations (Section 3.3). These values are based on experimental measurements performed by Lopez *et al.*[5]

We proceeded to compare the predictions of the proposed framework with results of controlled experiments performed by Miller *et al.*[3] In these experiments, three UVR exposure dose schedules, presented in Figure 8 (first column), were used to elicit skin tanning responses from a number of subjects (with ages varying from 22 to 65 years-old) characterized by low constitutive pigmentation levels (SPT II and III). Miller *et al.*[3] employed a Minolta CM-2002 spectrometer[58] to measure the subjects' skin reflectance during each visit. For each subject, three spectral reflectance readings were taken from each exposed area and averaged. The measured spectral reflectance data was then used to calculate the CIE $L^*a^*b^*$ color space coordinates considering a D65 illuminant.[56] We note that Miller *et al.*[3] provide as output data only L^* values, which they describe as the "quantity of reflected light weighted with the spectral responses of the human eye", indicating lightness.

To obtain predictions comparable to the data provided by Miller *et al.*,[3] we performed tanning dynamics simulations for a specimen with a low constitutive pigmentation level (Tables 1 to 3) using a virtual experimental setup analogous to the actual one (whose spatial arrangement is schematically illustrated in Figure 9) and the same UVR exposure doses employed by them. The resulting simulated physiological variations are presented in Figure 8 (second to fourth columns). This information was then used as input for the selected model of light and skin interactions in order to obtain modeled reflectance values. These, in turn, were employed to obtain CIE $L^*a^*b^*$ color space coordinates considering the same standard D65 illuminant used by Miller *et al.*[3] For the interested reader, more details about the skin color measurement setup employed by Miller *et al.*,[3] including the choice of standard illuminant, can be found in an earlier work[59] cited by them.

As it can be observed in Figure 8 (rightmost column), the simulated and measured values obtained for the lightness (L^*) coordinate show good agreement, especially considering the variations in the actual experiments

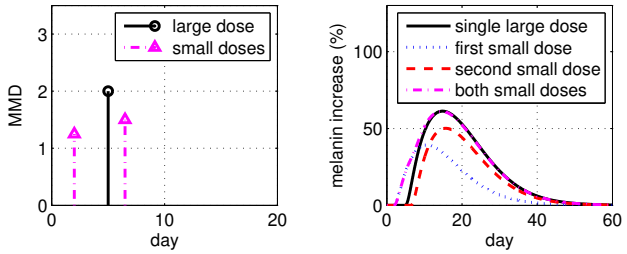

Figure 7: Simulated data illustrating the proposed framework's capability to account for the photoaddition phenomenon.[57] Left: two different UVR exposure dose schedules. Right: simulated melanin increase results provided by the proposed framework. The simulations were performed considering a specimen with low constitutive pigmentation level (Tables 1 to 3).

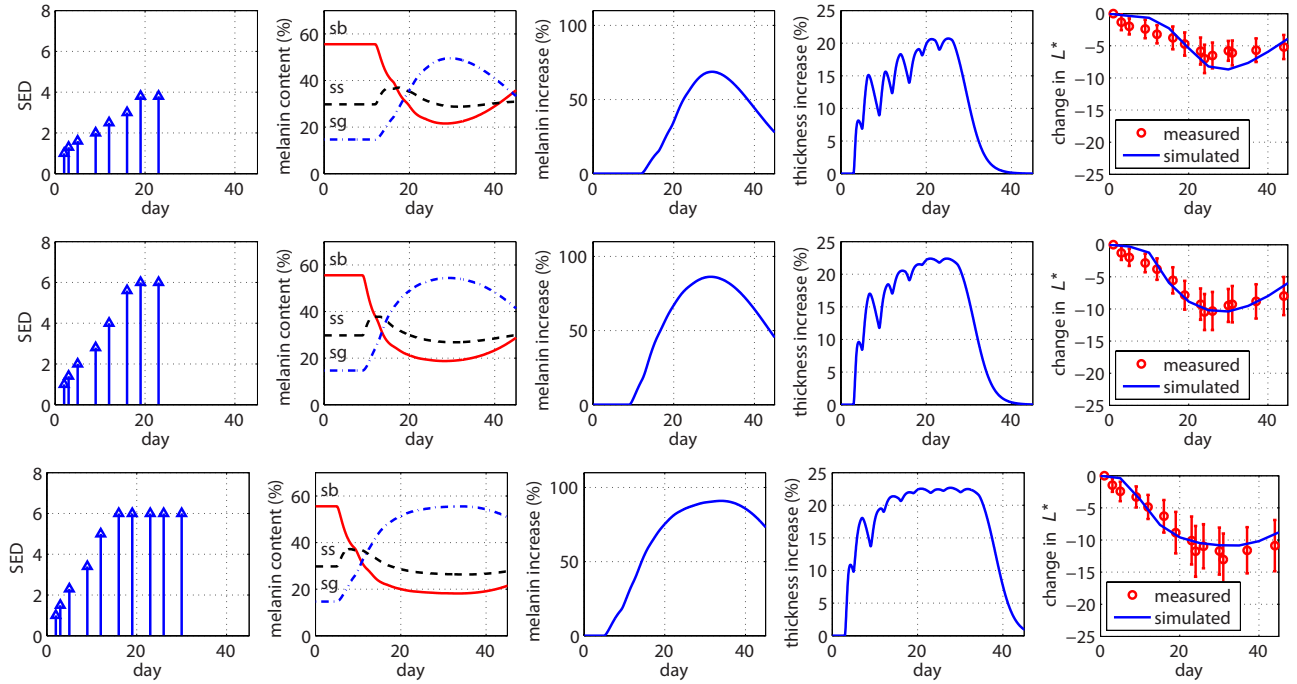

Figure 8: Simulated physiological variations resulting from three tanning processes triggered by three distinct UVR exposure dose schedules. First column: exposure dose schedules employed by Miller *et al.*[3] Second column: variations in relative melanin content, which is associated with this pigment's distribution in the different epidermal layers, namely stratum basale (sb), stratum spinosum (ss) and stratum granulosum (sg). Third column: variations in total melanin content. Fourth column: changes in skin thickness. Fifth column: comparisons of simulated results with measured values provided by Miller *et al.*[3] These comparisons are presented in terms of the change in the lightness L^* coordinate of the $L^*a^*b^*$ color space, with the bars depicting the standard deviations from the measured mean values indicated by the circles.

(indicated by error bars) associated with expected differences in the subjects' biophysical characteristics. In Figure 10, we present a sequence of images to illustrate the temporal visible appearance changes resulting from three UVR exposure schedules considered in these comparisons.

We remark that individuals with a high level of constitutive pigmentation have a higher MMD, *i.e.*, a higher UVR exposure dose is required to trigger their tanning processes.[2,47] Since they are less sensitive to UVR,[9] their appearance changes are less noticeable than those verified in individuals with lower constitutive pigmentation levels, considering both groups subjected to the same UVR exposure regime.[60] This behaviour is captured by the proposed framework as illustrated by the images presented in Figure 11. More specifically, it can be observed that

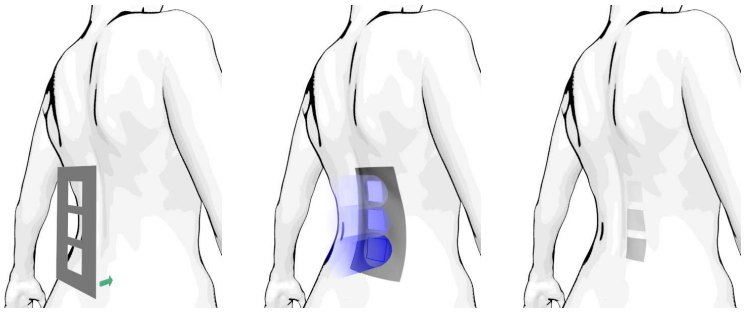

Figure 9: Artistic conception illustrating a standard experimental setup used for tanning experiments. A template is placed on the body (left) to isolate patches of skin in order to administer distinct measured UVR doses (center). The changes in these patches relating to different exposure doses (right) are then recorded.

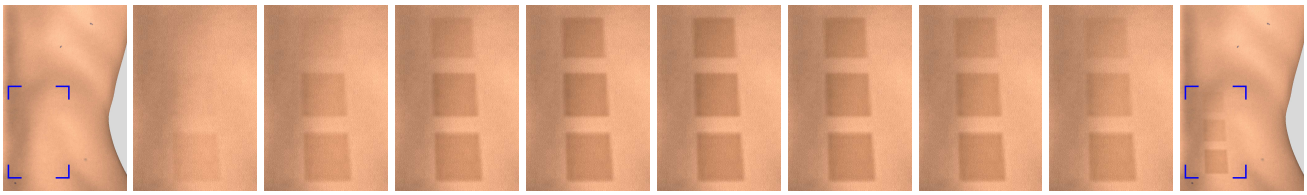

day 5 day 10 day 15 day 20 day 25 day 30 day 35 day 40 day 45 day 50

Figure 10: Sequence of images portraying the temporal changes in skin appearance as a result of the tanning processes described in Figure 8. The marked areas in the leftmost and rightmost images denote the boundaries of the in-between images. The top, middle and bottom tanned patches, in turn, correspond to the distinct exposure dose schedules provided in the top, middle and bottom rows of Figure 8, respectively.

the higher the constitutive pigmentation (darker native appearance) of a given specimen, the weaker the tanning responses that the specimen elicits. In fact, the lowest exposure dose schedule considered in our simulations is not sufficient to elicit a noticeable visible response in the darkest specimen (Figure 11 (right), top patch).

It is important to note that the increase in facultative pigmentation is more pronounced in individuals with high constitutive pigmentation levels than in those with low constitutive pigmentation levels, considering both groups exposed to UVR doses inversely proportional to their respective sensitivity to UVR (quantified in terms of MMD or MED).[9] As a result, a higher tanning ability is attributed to the former group of individuals.[3,32,60] This behaviour is also captured by the proposed framework as illustrated in the images presented in Figure 12. These images were obtained by scaling the exposure doses applied to the specimens with intermediate and high constitutive pigmentation levels by factors of 1.4 and 2.4, respectively. These factors are based on their distinct sensitivities to UVR verified in actual experiments.[25,51] As expected, the specimens with higher constitutive pigmentation levels show more noticeable appearance changes associated with stronger pigmentation build-ups.

It has also been demonstrated that different tanning abilities can be observed even among individuals with a similar level of constitutive pigmentation.[10] Accordingly, although individuals belonging to the SPT I, II, III and IV groups are all characterized by a low constitutive pigmentation level, SPT III and IV individuals have a higher tanning ability.[32,61] These trends are illustrated by the images presented in Figures 13 and 14. These images show appearance changes resulting from tanning processes triggered by the same UVR exposure regime (30 SED) applied to two individuals with a low constitutive pigmentation level, but different tanning abilities. As a result, the individual with a low tanning ability shows a lower pigmentation build-up 15 days after exposure, which can be observed by examining the appearance contrast between the untanned and tanned sides of this individual's face (Figure 13 (bottom left)). On the other hand, the individual with a high tanning ability shows a higher pigmentation build-up 15 days after exposure, which is particularly noticeable when one examines the appearance contrast provided by the tan lines left by the sunscreen (Figure 14 (right)).

The characteristic nonlinear appearance changes resulting from time-dependent tanning processes (triggered by a UVR exposure schedule equivalent to 30 SED) are further illustrated by an animation sequence (included in

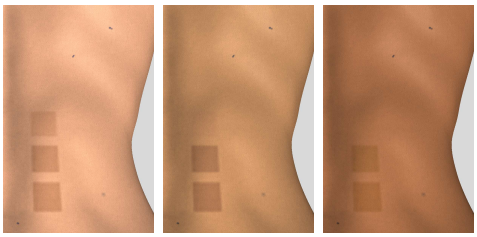

Figure 11: Images illustrating the distinct UVR sensitivities of specimens characterized by increasing levels of constitutive pigmentation, from low (left) to high (right), associated with skin phototypes III, IV and V, respectively. The same UVR exposure dose schedules presented in Figure 8 were applied to the specimens. The tanning responses depicted in the patches correspond to day 20, and they were obtained using the data provided in Tables 1 to 3.

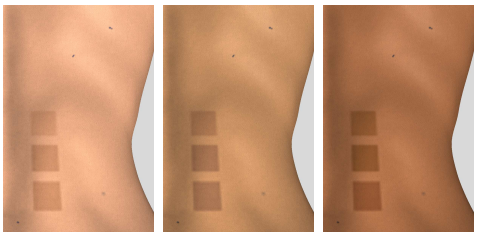

Figure 12: Images illustrating the different tanning abilities of specimens characterized by increasing levels of constitutive pigmentation, from low (left) to high (right), associated with skin phototypes III, IV and V, respectively. The same UVR exposure dose schedules presented in Figure 8 were applied to the specimens. The tanning responses depicted in the patches correspond to day 20, and they were obtained using the data provided in Tables 1 to 3. We note that the dose intensities were scaled by factors of 1.4 and 2.4 for the specimens with intermediate and high constitutive pigmentation levels, respectively, taking into account their UVR sensitivities.

the supplementary video*), with selected frames being presented in Figure 1. More specifically, one can notice a relatively rapid increase in pigmentation, reaching a broad maximum, which is then followed by a gradual fading. This behaviour is consistent with experimental observations on facultative pigmentation kinetics reported in the literature.[1,2,28] We note that, apart from its aesthetic implications, facultative pigmentation fading is also relevant to biomedical investigations since it may represent a reduction of natural photoprotection.[47]

It is worth mentioning that the sharpness of tan lines depends on the exposure conditions (duration, intensity and illumination geometry) and whether the tanned individual remained still during the exposure. The latter aspect also applies to the individual's clothes, shoes or any other object blocking the light. By taking different exposure conditions into account, one can obtain tan lines that suit the visual requirements of a given application. In the case of the animation whose frames are depicted in Figure 1, we assumed that the individual remained relatively still during the exposure.

Finally, we remark that the results of skin dynamics simulations can be translated to skin appearance attributes using different models of light and skin interactions. In the case of models in which the epidermis tissue is represented by a single layer, the values obtained for the modified skin biophysical parameters resulting from the simulations can be aggregated (Section 3.4) to accommodate the requirements of these models' parameter space. In order to illustrate this aspect, we have generated skin swatches (Figure 15) using the BioSpec model.[16] More specifically, this model was employed to translate the tanning data (updated melanin content and tissue thickness values) employed in the generation of the images presented in Figure 1 to skin appearance attributes (reflectance values from 400 to 700 nm, with a resolution of 5 nm). As mentioned in Section 3.4, these attributes were then converted to skin tone values using a standard XYZ to sRGB conversion procedure.[55] We note that the values initially assigned to the baseline skin biophysical parameters correspond to default values depicted on the website[62] made available for the online use of the BioSpec model.

*https://youtu.be/I1quYM34wWw

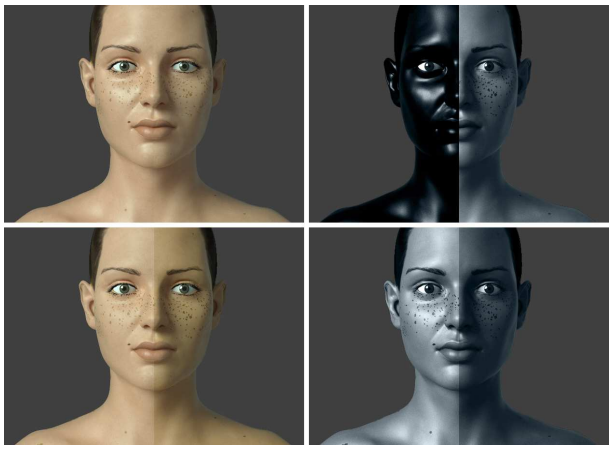

Figure 13: Images illustrating the visible skin appearance (left) and the corresponding ultraviolet appearance (right) of an individual with a low level of constitutive pigmentation and low tanning ability (SPT II) before and after a UVR exposure schedule equivalent to 30 SED. The top row depicts the pre-exposure appearance with an effective sunscreen applied to one side of the individual's face (depicting a glossier appearance). The bottom row depicts the appearance contrast between the untanned and tanned sides of the face 15 days after exposure. These images were generated using the data provided in Tables 1 (dataset $\mathcal{L}$), 2 and 3, and the ultraviolet appearance attributes (at 365 nm) are depicted using pseudo color.

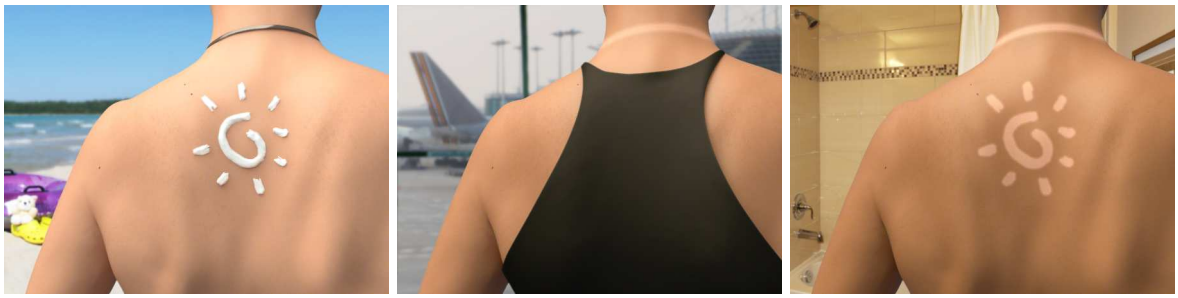

Figure 14: Sequence of images illustrating the appearance of an individual with a low level of constitutive pigmentation and high tanning ability (SPT III) before and after a UVR exposure schedule equivalent to 30 SED. Left: initial appearance just before sunbathing with an effective sunscreen applied on the individual's back as indicated. Center: noticeable darkening on the way home inside an airport 4 days after exposure. Right: significant darkening from a well developed tan as seen before taking a shower 15 days after exposure. To facilitate visual comparisons, the same illumination was used in the rendering of all three images. These images were generated using the data provided in Tables 1 (dataset $\mathcal{L}$, with $m_{p,i,f}$ of the stratum basale set to 0.0858), 2 and 3.

4.3 Practical Issues

To date, reflectance and BSSRDF datasets for human skin are relatively scarce in the scientific literature. The situation is even more critical when one searches for data for skin specimens under different tanning stages. The reflectance data is usually converted to colorimetric values, and those are only provided in a handful of works. We selected the three experimental test cases provided in the study by Miller *et al.*[3] because their controlled tanning experiments include more specific characterization data about the specimens (*e.g.*, skin phototype) in comparison with other studies involving skin tanning. In terms of BSSRDF data, to the best of our knowledge, there are still no available datasets for skin under different tanning stages.

Recall that the melanin and thickness dynamics simulations are preceded by a UVR dose evaluation procedure that calculates the UVR thresholds and intakes required to activate the melanogenesis and hyperplasia

Figure 15: Sequence of skin swatches obtained using the BioSpec model[16] to translate simulation results (employed in the generation of the images presented in Figure 1) to skin appearance attributes. The top areas represent the untanned portion of the skin specimen, while the bottom areas depict its appearance before (day 0) and after a UVR exposure schedule equivalent to 30 SED.

mechanisms in a given specimen. These calculations employ spectral absorptance values that are computed using a model of light and skin interactions. Hence, the time spent on this procedure depends on the performance of the selected model. We note, however, that if suitable data for the specimen of interest is available (*e.g.*, MMD, MED and exposure doses given in terms of SED), then the calculations performed in the UVR dose evaluation procedure can be replaced by the direct input of this measured data to the framework. In the absence of such measured data, one could instead resort to the pre-computation of the required absorptance values. The results of these computations would then be accessed on demand during the UVR dose evaluations. We remark that HyLIoS, the model employed in this research, has been made available[49] for use in such standalone applications. Considering the execution of the framework's two dynamics components using pre-computed spectral absorptance values, it takes less than a hundredth of a second on a 2.6 GHz dual-core Intel i5 cpu-based machine to compute the changes in biophysical parameters for a time period of a year at a temporal resolution of one hour.

5. CONCLUSION AND FUTURE WORK

In this paper, we have described the first comprehensive physiologically-based framework for the simulation and visualization of skin tanning dynamics presented in the scientific literature.[6] It incorporates UVR-dependent and time-dependent algorithms for the predictive simulation of stimulus-response mechanisms leading to nonlinear changes in skin appearance over time. Moreover, it enables the predictive simulation of tanning effects on individuals with different biophysical characteristics and subjected to distinct UVR exposure conditions. The results of these simulations can then be used in the production of computer visualizations depicting environmentally-dependent variations on skin appearance. Such visualizations are of interest to a broad spectrum of investigations carried out in a diverse array of fields, from biology and medicine to biomedical photonics and computer graphics.

Having predictability as its main guideline, the proposed framework can potentially be used to support interdisciplinary research initiatives involving the appearance and health status of human skin. Examples of such initiatives include, but are not limited to, the evaluation of hypotheses about the photoprotection offered by different facultative pigmentation levels, the development of interactive platforms for the education of the general public about the harmful effects of excessive UVR exposure on skin health, and the *in silico* testing of products, such as lotions and sunscreens, aimed at protecting individuals against these effects.

We remark that the skin on virtual characters employed in computer graphics applications (*e.g.*, movies and games) is usually considered to be independent from the surrounding digital setting, *i.e.*, the causal relationships between environmental stimuli and skin appearance changes are largely overlooked. The proposed framework can be used to predictively address this limitation.

At this stage of our work, we focused on the predictive reproduction of dynamical changes in skin appearance. Accordingly, we elected to provide a detailed parameter space for the proposed framework so that researchers can experiment with a wide range of biophysical variables. However, this parameter space can be made more compact and accessible via interfaces tailored to animation production pipelines. This would facilitate the incorporation of the proposed framework in image synthesis systems employed in computer graphics applications.

As future work, we plan to investigate phenomena leading to transient tanning responses. For example, soon after UVR exposure, skin might exhibit a subtle darkening that has been suggested to be a result of physicochemical processes.[27] Although the direct influence of these phenomena on skin appearance is minimal,

their simulation may provide important clues with respect to the onset of pathological conditions that can seriously disrupt skin's photoprotection mechanisms.

REFERENCES

[1] M. Brenner and V.J. Hearing, "The protective role of melanin against UV damage in human skin," *Photochem. Photobiol.*, vol. 84, no. 3, pp. 539–549, 2008.

[2] M.H. Ravnbak, P.A. Philipsen, S.R. Wiegell, and H.C. Wulf, "Skin pigmentation kinetics after UVB exposure.," *Acta Derm. Venereol.*, vol. 88, no. 3, pp. 223–228, 2008.

[3] S.A. Miller, S.G. Coelho, S.W. Miller, Y. Yamaguchi, V.J. Hearing, and J.Z. Beer, "Evidence for a new paradigm for ultraviolet exposure: a universal schedule that is skin phototype independent," *Photodermatol. Photoimunol. Photomed.*, vol. 28, no. 4, pp. 187–195, 2012.

[4] T.F. Chen, G.V.G. Baranoski, B.W. Kimmel, and E. Miranda, "Hyperspectral modeling of skin appearance," *ACM T. Graphic.*, vol. 34, no. 3, pp. 31:1–31:14, 2015.

[5] H. Lopez, Z.J. Beer, S.A. Miller, and B.Z. Zmudzka, "Ultrasound measurements of skin thickness after UV exposure: a feasibility study," *J. of Photochem. Photobiol. B*, vol. 73, no. 3, pp. 123–132, 2004.

[6] T.F. Chen, *On the Modelling of Hyperspectral Light and Skin Interactions and the Simulation of Skin Appearance Changes Due to Tanning*, Ph.D. thesis, Natural Phenomena Simulation Group, David R. Cheriton School of Computer Science, University of Waterloo, Canada, December 2015.

[7] J. Thingnes, L. Oyehaug, E. Hovig, and S. Omholt, "The mathematics of tanning," *BMC Syst. Biol.*, vol. 3, no. 1, pp. 60, 2009.

[8] J. Thingnes, L. Oyehaug, and E. Hovig, "Mathematical and biological processes of skin pigmentation," in *Computational Biosphysics of the Skin*, B. Querleux, Ed., pp. 3–24. Pan Stanford Pub., Singapore, 2014.

[9] S.A. Miller, S.G. Coelho, B.Z. Zmudzka, and J.Z. Beer, "Reduction of the UV burden to indoor tanners through new exposure schedules: a pilot study," *Photodermatol. Photoimunol. Photomed.*, vol. 22, no. 2, pp. 59–66, 2006.

[10] M.H. Ravnbak, *Objective determination of Fitzpatrick skin type*, Ph.D. thesis, University of Copenhagen, Denmark, 2010.

[11] J.A. Parrish, K.F. Jaenicke, and R.R. Anderson, "Erythema and melanogenesis action spectra of normal human skin," *Photochem. Photobiol.*, vol. 36, no. 2, pp. 187–191, 1982.

[12] S. López, S. Alonso, A.G. Galdeano, and I. Smith-Zubiaga, "Melanocytes from dark and light skin respond differently after ultraviolet B irradiation: effect of keratinocyte-conditioned medium," *Photodermatol. Photoimmunol. Photomed.*, vol. 31, pp. 149–158, 2015.

[13] A.D. Pearse, S.A. Gaskell, and R. Marks, "Epidermal changes in human skin following irradiation with either UVB or UVA," *J. Invest. Dermatol.*, vol. 88, no. 1, pp. 83–87, 1987.

[14] T.S.C. Poon, J.M. Kuchel, A. Badruddin, G.M. Halliday, R.S. Barnetson, H. Iwaki, and M. Hatao, "Objective measurement of minimal erythema and melanogenic doses using natural and solar-simulated light," *Photochem. Photobiol.*, vol. 78, no. 4, pp. 331–336, 2003.

[15] G.V.G. Baranoski and A. Krishnaswamy, *Light & Skin Interactions: Simulations for Computer Graphics Applications*, Morgan Kaufmann/Elsevier, Burlington, MA, USA, 2010.

[16] A. Krishnaswamy and G.V.G. Baranoski, "A biophysically-based spectral model of light interaction with human skin," *Comput. Graph. Forum*, vol. 23, no. 3, pp. 331–340, 2004.

[17] G.V.G. Baranoski, A. Dey, and T. F. Chen, "Assessing the sensitivity of human skin hyperspectral responses to increasing anemia severity levels," *J. Biomed. Opt.*, vol. 20, no. 9, pp. 095002:1–14, 2015.

[18] G.V.G Baranoski, S.R. Van Leeuwen, and T.F. Chen, "Elucidating the biophysical processes responsible for the chromatic attributes of peripheral cyanosis," in *39th Annual International Conference of the IEEE Engineering in Medicine and Biology Society (EMBC)*, Jeju, South Korea, August 2017, pp. 90–95.

[19] G.V.G Baranoski, S.R. Van Leeuwen, and T.F. Chen, "On the detection of peripheral cyanosis in individuals with distinct levels of cutaneous pigmentation," in *39th Annual International Conference of the IEEE Engineering in Medicine and Biology Society (EMBC)*, Jeju, South Korea, August 2017, pp. 4260–4264.

[20] S.W. Askew and G.V.G. Baranoski, "On the dysfunctional hemoglobins and cyanosis connection: Practical implications for the clinical detection and differentiation of methemoglobinemia and sulfhemoglobinemia," *Biomed. Opt. Express*, vol. 9, no. 1, pp. 3284–3305, 2018.

[21] G.V.G Baranoski, T.F. Chen, and S.R. Van Leeuwen, "On the effective differentiation and monitoring of variable degrees of hyperbilirubinemia severity through noninvasive screening protocols," in *40th Annual International Conference of the IEEE Engineering in Medicine and Biology Society (EMBC)*, Honolulu, HI, USA, July 2018, pp. 6153–6157.

[22] N. Magnenat-Thalmann, P. Kalra, J.L. Lévêque, R. Bazin, D. Batisse, and B. Querleux, "A computational skin model: fold and wrinkle formation," *IEEE Trans. Inf. Technol. B.*, vol. 6, no. 4, pp. 317–323, 2002.

[23] R.S. Barros and M. Walter, "Synthesis of human skin pigmentation disorders," *Comput. Graph. Forum*, vol. 36, no. 1, pp. 330–344, 2016.

[24] J.A. Iglesias-Guitian, C. Aliaga, A. Jarabo, and D. Gutierrez, "A biophysically-based model of the optical properties of skin aging," *Comput. Graph. Forum*, vol. 34, no. 2, pp. 45–55, 2015.

[25] T. Tadokoro, Y. Yamaguchi, J. Batzer, S.G. Coelho, B.Z. Zmudzka, S.A. Miller, R. Wolber, J.Z. Beer, and V.J. Hearing, "Mechanisms of skin tanning in different racial/ethnic groups in response to ultraviolet radiation," *J. Investig. Dermatol.*, vol. 124, no. 6, pp. 1326–1332, 2005.

[26] B.A. Gilchrest, H. Park, M.S. Eller, and M. Yaar, "Mechanisms of ultraviolet light-induced pigmentation," *Photochem. Photobiol.*, vol. 63, no. 1, pp. 1–10, 1996.

[27] Y. Miyamura, S.G. Coelho, R. Wolber, S.A. Miller, K. Wakamatsu, B.Z. Zmudzka, S. Ito, C. Smuda, T. Passeron, W. Choi, J. Batzer, Y. Yamaguchi, J.Z. Beer, and V.J. Hearing, "Regulation of human skin pigmentation and responses to ultraviolet radiation," *Pigm. Cell Res.*, vol. 20, no. 1, pp. 2–13, 2006.

[28] J.L.M. Hawk and J.A. Parrish, "Responses of normal skin to ultraviolet radiation," in *The Science of Photomedicine*, James D. Regan and John A. Parrish, Eds., chapter 8. Plenum Press, 1982.

[29] G.J. Clydesdale, G.W. Dandie, and H.K. Muller Konrad, "Ultraviolet light induced injury: immunological and inflammatory effects," *Immunol. Cell. Biol.*, vol. 79, no. 6, pp. 547– 568, 2001.

[30] P. Agache, "Assessment of erythema and pallor," in *Measuring the Skin*, P. Agache and P. Humbert, Eds. 2004, pp. 591–601, Springer.

[31] G.V.G Baranoski and T.F. Chen, "On the identification and interpretation of human skin spectral responses under adverse environmental conditions," in *37th Annual International Conference of the IEEE Engineering in Medicine and Biology Society (EMBC)*, Milan, Italy, August 2015, pp. 845–848.

[32] M.A. Pathak, "Functions of melanin and protection by melanin," in *Melanin: Its Role in Human Photoprotection*, M.R. Chedekel L. Zeise and T.B. Fitzpatrick, Eds., Overland Park, Kansas, USA, 1995, pp. 125–134, Valdenmar Publishing Co.

[33] R.R. Anderson and J.A. Parrish, "Optical properties of human skin," in *The Science of Photomedicine*, J.D. Regan and J.A. Parrish, Eds., N.Y., USA, 1982, pp. 147–194, Plenun Press.

[34] M.R. Chedekel, "Photophysics and photochemistry of melanin," in *Melanin: Its Role in Human Photoprotection*, M.R. Chedekel L. Zeise and T.B. Fitzpatrick, Eds., Overland Park, Kansas, USA, 1995, pp. 11–22, Valdenmar Publishing Co., 2223b.

[35] C.C. Cooksey and D.W. Allen, "Reflectance measurements of human skin from the ultraviolet to the shortwave infrared (250 nm to 2500 nm)," in *Proc. of SPIE, Active and Passive Signatures IV*, G.C. Gilbreath and C.T. Hawley, Eds., 2013, vol. 8734, pp. 87340N–1–9.

[36] C. Routaboul, A. Denis, and A. Vinche, "Immediate pigment darkening: description, kinetic and biological function," *Eur. J. Dermatol.*, vol. 9, no. 2, pp. 95–99, 1999.

[37] S.G. Coelho, W. Choi, M. Brenner, Y. Miyamura, Y. Yamaguchi, R. Wolber, C. Smuda, J. Batzer, L. Kolbe, S. Ito, K. Wakamatsu, B.Z. Zmudzka, J.Z. Beer, S.A. Miller, and V.J. Hearing, "Short- and long-term effects of UV radiation on the pigmentation of human skin," *J. Invest. Dermatol.*, vol. 14, pp. 32–35, 2009.

[38] T.F. Chen and G.V.G Baranoski, "Melanosome distribution patterns affecting skin reflectance: implications for the in vivo estimation of epidermal melanin content," in *International Conference of the IEEE Engineering in Medicine and Biology Society (EMBC)*, Italy, 2015, pp. 4415–4418.

[39] G.V.G Baranoski, T.F. Chen, and P. Varsa, "Unveiling the impact of distinct melanosome arrangements on the attenuation of cancer-inducing ultraviolet radiation," in *40th Annual International Conference of the IEEE Engineering in Medicine and Biology Society (EMBC)*, Honolulu, HI, USA, July 2018, pp. 4981–4986.

[40] N. Kollias, R.M. Sayre, L. Zeise, and M.R. Chedekel, "Photoprotection by melanin," *J. Photoch. Photobio. B.*, vol. 9, no. 2, pp. 135–60, 1991.

[41] G. Costin and V.J. Hearing, "Human skin pigmentation: melanocytes modulate skin color in response to stress," *The FASEB Journal*, vol. 21, no. 4, pp. 976–994, 2007.
[42] H.C. Wulf, P.A. Philipsen, and M.H. Ravnbak, "Minimal erythema dose and minimal melanogenesis dose relate better to objectively measured skin type than to Fitzpatricks skin type," *Photodermatol. Photoimmunol. Photomed.*, vol. 26, no. 6, pp. 280–284, 2010.
[43] W.M. Star, "Light dosimetry *in vivo*," *Phys. Med. Biol.*, vol. 42, no. 5, pp. 763, 1997.
[44] International Programme on Chemical Safety, "Environmental health criteria (EHC) 160: Ultraviolet radiation," Tech. Rep., World Health Organization, 1994.
[45] A. Anders, H. Altheide, M. Knälmann, and H. Tronnier, "Action spectrum for erythema in humans investigated with dye lasers," *Photochem. Photobiol.*, vol. 61, no. 2, pp. 200–205, 1995.
[46] J. Lock-Andersen, H.C. Wulf, and N.M. Mortensen, "Erythemally weighted radiometric dose and standard erythema dose (SED)," in *12th International Congress on Photobiology*, Vienna, Austria, 1996, Later published in "Landmarks in Photobiology", H. Hönigsman, R.M. Knobler, F. Trautinger and G. Jori Eds., Milan: Organizzazione Editoriale Medico, 1998, pp. 315-317.
[47] M.H. Ravnbak, P.A. Philipsen, S.R. Wiegell, and H.C Wulf, "Skin pigmentation kinetics after exposure to ultraviolet A," *Acta Derm. Venereol.*, vol. 89, no. 4, pp. 357–363, 2009.
[48] A.F. Mckinlay and B.L. Diffey, "A reference action spectrum for ultraviolet induced erythema in human skin," *CIE J.*, vol. 6, no. 1, pp. 17–22, 1987.
[49] NPSG, *Run HyLIoS Online*, Natural Phenomena Simulation Group (NPSG), School of Computer Science, University of Waterloo, Ontario, Canada, 2014, http://www.npsg.uwaterloo.ca/models/hyliosEx.php.
[50] S.R. Van Leeuwen and G.V.G Baranoski, "Elucidating the contribution of Rayleigh scattering to the bluish appearance of veins," *J. Biomed. Opt.*, vol. 23, no. 2, pp. 025001–1–17, 2018.
[51] M.H. Ravnbak, P.A. Philipsen, and H.C. Wulf, "The minimal melanogenesis dose/minimal erythema dose ratio declines with increasing skin pigmentation using solar simulator and narrowband ultraviolet B exposure," *Photodermatol. Photoimunol. Photomed.*, vol. 26, no. 3, pp. 133–137, 2010.
[52] L.S. Sklar, F. Almutawa, H.W. Lim, and I. Hamzavi, "Effects of ultraviolet radiation, visible light, and infrared radiation on erythema and pigmentation: a review," *Photochem. Photobiol. Sci.*, vol. 12, pp. 54–64, 2013.
[53] A. Hennessy, C. Oh, B. Diffey, K. Wakamatsu, S. Ito, and J. Rees, "Eumelanin and pheomelanin concentrations in human epidermis before and after UVB irradiation," *Pigm. Cell Res.*, vol. 18, pp. 220–223, 2005.
[54] S. Goutelle, M. Maurin, F. Rougier, X. Barbaut, L. Bourguignon, M. Ducher, and P. Maire, "The Hill equation: a review of its capabilities in pharmacological modelling," *Fund. Clin. Dermatol.*, vol. 22, pp. 633–648, 2008.
[55] M.C. Stone, *A Field Guide to Digital Color*, AK Peters, Natick, MA, USA, 2003.
[56] N. Ohta and A.R. Robertson, *Colorimetry Fundamentals and Applications*, John Wiley & Sons, New York, NY, USA, 1982.
[57] M. Spencer and R.A. Amonette, "Indoor tanning: risks, benefits, and future trends," *J. Am. Acad. Dermatol.*, vol. 33, no. 2, pp. 288–298, 1995.
[58] P. Blum, "Reflectance spectrophotometry and colorimetry," in *Physical Properties Handbook*. 1997, pp. 7:1–11, International Ocean Discovery Program, Technical Note 26, Chapter 7.
[59] A. Fullerton, T. Fischer, A. Lahti, K. Wilhelm, T. Takiwaki, and J. Serup, "Guidelines for measurement of skin colour and erythema," *Contact Dermatitis*, vol. 35, pp. 1–10, 1996.
[60] A. Pezic, A. Ponsonby, F.J. Cameron, C. Rodda, J.A. Ellis, J. Halliday, W. Siero, R.M. Lucas, and T. Dwyer, "Constitutive and relative facultative skin pigmentation among Victorian children including comparison of two visual skin charts for determining constitutive melanin density," *Photochem. Photobiol.*, vol. 89, pp. 714–723, 2013.
[61] J. Lock-Andersen, N.D. Knudstorp, and H.C. Wulf, "Facultative skin pigmentation in Caucasians: an objective biological indicator of lifetime exposure to ultraviolet radiation?," *Brit. J. Dermatol.*, vol. 138, pp. 826–832, 1998.
[62] NPSG, *Run BioSpec Online*, Natural Phenomena Simulation Group (NPSG), School of Computer Science, University of Waterloo, Ontario, Canada, 2010, http://www.npsg.uwaterloo.ca/models/biospec.php.